Front. Med. 2016, 10(3): 286–296
DOI 10.1007/s11684-016-0456-9

RESEARCH ARTICLE

Influence of the intensity and loading time of direct current electric field on the directional migration of rat bone marrow mesenchymal stem cells

Xiaoyu Wang[1], Yuxuan Gao[1], Haigang Shi[2], Na Liu[1], Wei Zhang[2], Hongbo Li (✉)[1]

[1]*Department of Stomatology, Chinese PLA General Hospital, Beijing 100853, China;* [2]*Technical Institute of Physics and Chemistry, Chinese Academy of Sciences, Beijing 100190, China*

Abstract **Exogenic electric fields can effectively accelerate bone healing and remodeling through the enhanced migration of bone marrow mesenchymal stem cells (BMSCs) toward the injured area. This study aimed to determine the following: (1) the direction of rat BMSC (rBMSC) migration upon exposure to a direct current electric field (DCEF), (2) the optimal DCEF intensity and duration, and (3) the possible regulatory role of SDF-1/CXCR4 axis in rBMSC migration as induced by DCEF. Results showed that rBMSCs migrated to the positive electrode of the DCEF, and that the DCEF of 200 mV/mm for 4 h was found to be optimal in enhancing rBMSC migration. This DCEF strength and duration also upregulated the expression of osteoblastic genes, including ALP and OCN, and upregulated the expression of ALP and Runx2 proteins. Moreover, when CXCR4 was inhibited, rBMSC migration due to DCEF was partially blocked. These findings indicated that DCEF can effectively induce rBMSC migration. A DCEF of 200 mV/mm for 4 h was recommended because of its ability to promote rBMSC migration, proliferation, and osteogenic differentiation. The SDF-1/CXCR4 signaling pathway may play an important role in regulating the DCEF-induced migration of rBMSCs.**

Keywords DCEF; migration; osteogenesis differentiation; rBMSCs; SDF-1/CXCR-4

Introduction

Bone defects are serious complications commonly caused by extensive trauma, tumors, infections, or genetic diseases. The clinical outcomes of current methods used to enhance bone healing and remodeling are unsatisfactory. In addition to improving surgical techniques and the development of better bone-repair and bone-substitute materials, adopting cytokines and physicochemical stimulations can also effectively accelerate bone healing and remodeling.

Bone tissue reconstruction and healing involve complex biological and biomechanical mechanisms requiring the integrated function of bone marrow mesenchymal stem cells (BMSCs), osteoblasts, osteoclasts, and other cells in the injured region. These mechanisms also depend on the recruitment of BMSCs, which are key players in bone healing, from surrounding tissue and the whole body to the injured area, as well as on their subsequent proliferation and osteogenic differentiation [1]. Therefore, the development of effective methods to enhance BMSC migration to an injured area is a research hotspot in the field of bon-tissue repair.

An endogenous biological electric field (EF), usually ranging from 10 to 200 mV/mm, is generated at the site of trauma following an injury [2]. It plays an essential role in the healing process, and an inhibition of EF leads to delayed tissue repair [3,4]. Galvanotaxis occurs in a variety of cells, including BMSCs. Cellular functions in different regions of the wound surface are positively correlated with the distribution of the biological EF intensity. Moreover, this EF is time dependent, gradually attenuates, and eventually disappears during the healing process. It has been proven that applied direct current electric field (DCEF) can enhance both the quality and quantity of bone healing *in vivo* [5]. Both the duration and intensity of exogenous DCEF have better controllability and can significantly improve the biological functions of BMSCs.

Received February 9, 2016; accepted May 5, 2016
Correspondence: hongbolii@sina.com

Thus, exogenous DCEF promotes the formation of bone tissue during bone repair, the initial process of which is the recruitment of BMSCs into the injured area [6].

As to the galvanotaxis patterns, cells of various types respond quite differently to applied EF. Rat osteoblasts, bovine aortic vascular endothelial cells, human BMSCs, bovine chondrocytes, and mouse endothelial progenitor cells tend to migrate toward the negative electrode [7]. Conversely, the migrations of human osteosarcoma cells, human umbilical vein endothelial cells, rabbit corneal endothelial cells, and rabbit osteoclasts are toward positive electrode. However, there are also studies with conflicting viewpoints [8]. Additionally, the migrating direction of BMSCs exposed to DCEF, which is an essential piece of information for clinical and nonclinical studies, is not yet determined. The optimal values for the voltage and duration of DCEF also need to be determined for both scientific research and clinical applications. However, investigations in this field are very limited. Some studies suggest a DCEF of 100 mV/mm because it is closer to the physiological value and similar to the strength of the endogenous wound EFs (~42–100 mV/mm) [9]. Other studies showed that cellular migration peaked at 300 mV/mm. Zhao *et al.* found that a DCEF of 200 mV/mm for 2 h was optimal for human BMSCs using the agar salt bridge electric generator and nuclei tracing method [10].

The mechanisms involved in the electrotaxis of BMSCs are not fully understood. Several intracellular signaling pathways or cytokines may mediate the DCEF-induced cell migration including PI3 kinase, PTEN, EGFR-ERK1/2, integrins-Rac pathways, cAMP, and Rho small GTPases [11–14]. The SDF-1/CXCR4 axis plays an important role in stem cell migration by mobilizing BMSCs from the bone marrow into the peripheral circulation [15]. BMSCs can produce SDF-1 and CXCR4, both of which are regulators of homing and proliferation. These data strongly suggest that the SDF-1/CXCR4 axis may be an important factor in DCEF-induced BMSCs migration.

Therefore, the aims of this study were to explore the direction of rat BMSC (rBMSC) migration upon exposure to DCEF, to test the optimal intensity and loading time of the DCEF to facilitate migration, and to determine the relationship between SDF-1/CXCR4 axis and BMSC migration when exposed to DCEF.

Materials and methods

The research strategy is shown in Fig. 1.

Cell cultures and characterization

Study subjects were male Sprague-Dawley (SD) rats (aged 3 weeks) that were purchased from Beijing HFK Bioscience Co. Ltd., Beijing, China. All animal care procedures conform to the principle of the Guidance Suggestions for the Care and Use of Laboratory Animals promulgated by the Ministry of Science and the Animal Care and Use Committee of Chinese PLA (People's Liberty Army) General Hospital, Beijing, China. All animals were housed in individual cages in a room with a temperature of 21–25 °C and a humidity of 45% to 50%

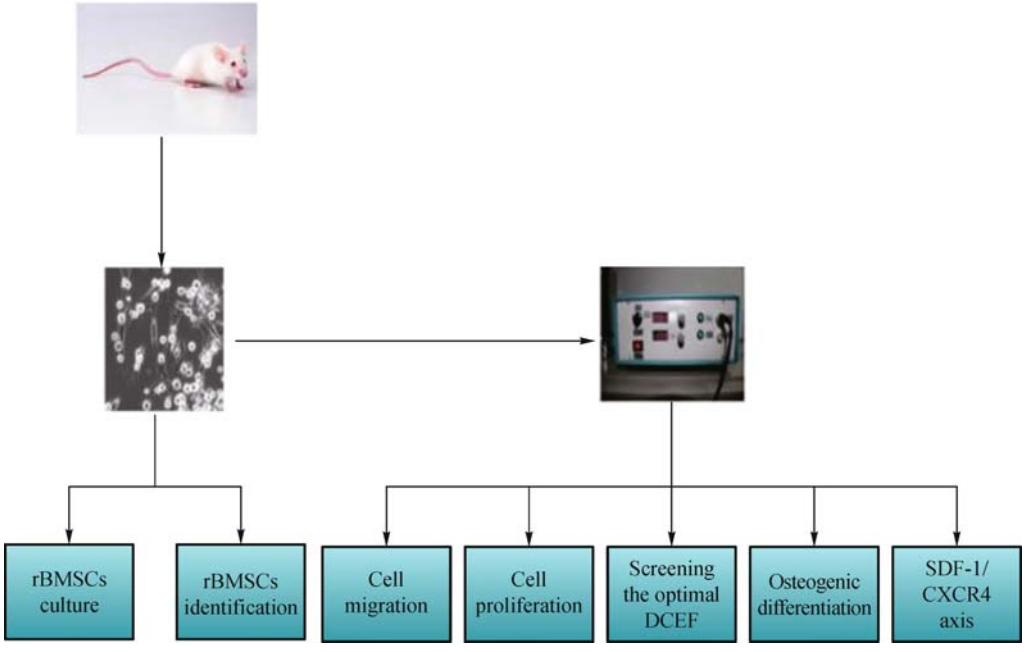

Fig. 1 Experimental design and process.

with a 12-h light/dark cycle and *ad libitum* access to pellet chow and water. The rats were sacrificed by an overdose of anesthesia. Primary cultures of rBMSCs were obtained by flushing the bone marrow from the tibias of SD rats. The cells were seeded on a 50-cm^2 culture flask in Dulbecco's Modified Eagle Medium (DMEM) supplemented with 10% fetal bovine serum and 1% penicillin-streptomycin at 37 °C in an incubator with 5% CO_2. The cells were fed every 2 days and were maintained in primary culture for 5 to 6 days. After the cells reached confluence, they were trypsinized and placed in new culture plates. Cells in the third passage were used for the experiments. For immunostaining, the cells were washed twice in phosphate-buffered saline (PBS) and incubated with rat monoclonal antibodies, anti-CD146 (ab203118, Abcam, USA), anti-stro-1 (sc47733, Santa Cruz Biotech, USA), anti-CD90 (ab92574, Abcam, USA), anti-CD34 (ab81289, Abcam, USA), anti-CD44 (ab81289, Abcam, USA), anti-CD29 (No. 4706, CST, USA), or anti-CD45 (No. 13917, CST, USA) primary antibodies. The researchers used goat anti-rabbit IgG H&L Alexa Fluor 488 (ab150077, Abcam, USA) as the secondary antibody. The immunostained cells were analyzed using flow cytometry with a Beckman Coulter Epics XL flow cytometer (Beckman Coulter, Fullerton, CA, USA).

Electrical stimulation

The loading device is an external DCEF generator providing constant direct current to two wires, each connected to a copper electrode plate. The electrode plates have a uniform thickness of 1 mm and are of the same size as the culture dishes. A sterilized electrode plate is placed both at the top and at the bottom of the culture dish, and the whole arrangement is placed in the incubator. The voltage is regulated by adjusting the distance between the two electrode plates, thus determining the DCEF intensity.

The Transwell migration assay

Cell migration was evaluated using a modified Boyden chamber, which consists of a 24-well plate containing Transwell inserts (polycarbonate membrane inserts 6.5 mm in diameter, containing 8.0-μm pores; Corning, Schiphol, Netherlands). Cells (4×10^5 cells/ml) were seeded 150 μl/well, and allowed to attach and stretch for at least 24 h in the upper chambers in DMEM (supplemented with 10% fetal bovine serum (FBS) and 1% penicillin-streptomycin) at 37 °C in a 5% CO_2 incubator. The cells were counted in at least five randomly selected microscopic fields. Data was expressed as the average number of migrating cells for each condition obtained from three independent experiments. Then, nonmigrating cells were removed from the top chamber, and migrated cells were fixed in methanol and stained with 4,6-diamidino-2-phenylindole (DAPI) (Sigma, USA).

Direction of rBMSCs migration

A DCEF of 200 mV/mm for 4 h was applied to the modified Boyden chambers by attaching the positive electrode and negative electrode to the upper and lower chambers. Three groups were established: the group without DCEF (A1), the group (A2) with positive electrode at the top and negative electrode at the bottom, and the group (A3) with negative electrode at the top and positive electrode at the bottom (Table 1).

Table 1 Direction of rBMSCs migration

Direction	Group		
	A1	A2	A3
Top	–	Positive electrode	Negative electrode
Bottom	–	Negative electrode	Positive electrode

Optimization of DCEF intensity and loading time

Twelve groups were established, of which nine groups were exposed to DCEF and three control groups were not. The loading time of DCEF ranged from 0 to 6 h, and the intensity of the DCEF ranged from 0 to 300 mV/mm. The upper chambers were seeded with rBMSCs (4×10^5/ml) resuspended in DMEM containing 2% FBS from each group. After 24 h, the nonmigrating cells were removed, and the migrating cells were stained with DAPI.

The function of SDF-1/CXCR4 in rBMSC migration

The Transwell assay was used to demonstrate the function of SDF-1/CXCR4 in rBMSC migration. Six groups of rBMSCs were established and cultured in DMEM containing 10% FBS, with three variable factors: SDF-1, AMD3100 (5 μg/ml), and the optimum DCEF (Table 2).

Cell proliferation and differentiation

MTT assay

For the 3-(4,5-dimethylthiazol-2-yl)-2,5-diphenyltetrazolium bromide (MTT) assay, rBMSCs were plated in 96-well culture plates (5×10^6 cells/well) in DMEM supplemented with 10% FBS. rBMSCs were divided into two groups: one group was exposed to DCEF at the

Table 2 Electric field has enhanced effect of SDF-1

Group	B1	B2	B3
Upper chamber	rBMSCs	rBMSCs	rBMSCs
Lower chamber	DMEM	DMEM + SDF-1	DMEM + SDF-1 + AMD3100
Group	B4	B5	B6
Upper chamber	rBMSCs + DCEF	rBMSCs + DCEF	rBMSCs + DCEF
Lower chamber	DMEM	DMEM + SDF-1	DMEM + SDF-1 + AMD3100

optimum intensity and duration, while another one was set as a control with no DCEF exposure. The MTT assay was carried out every day for 7 days according to the cell proliferation kit protocol (5 mg/ml PBS, pH 7.4, Sigma). Following the MTT assay, the absorbance in each well was measured at 490 nm using the iMark Microplate Absorbance Reader (Bio-Rad Laboratories, Hercules, CA, USA). These experiments were repeated three times.

Flow cytometry

The same groups of cells were used as shown in MTT assay, cells were resuspended into a monoplast suspension at a concentration of 5×10^5 cells/ml, centrifuged at 800 r/min for 5 min and washed twice using ice-cold PBS. The supernatant was collected, and the cells were fixed using ice-cold 75% ethanol for at least 4 h at 4 °C. The cells were then centrifuged at 1500 r/min for 5 min, and the supernatant was discarded. The pellet was washed once in 3 ml of PBS and incubated with 400 μl of ethidium bromide (PI, 50 μg/ml) and 100 μl of RNase A (100 μg/ml) in the dark for 30 min at 4 °C. A standard program in the flow cytometry instrument was calibrated and tested to count 20 000 – 30 000 cells, and the results from the cell counts were analyzed using a cell cycle and ModFit analysis software.

Osteogenic differentiation

Initially, rBMSCs were cultured in a growth medium containing DMEM with 10% FBS and 1% penicillin-streptomycin. Four experimental groups were established with two variable factors: DCEF and osteogenesis-induced liquid (OIF) (Table 3). The cells were plated in 24-well plates at a density of 6000 cells/well (~2 cm^2) for osteogenic differentiation. The culture medium was changed every other day, and cells were maintained for 4 weeks, followed by washing with PBS and fixation in 4% paraformaldehyde solution. The fixed cells were stained for BCIP/NBT Alkaline Phosphatase Color Development Kit (Beyotime C3206), which used BCIP/NBT as a phosphatase substrate; it turned blue when dephosphorylated by ALP. Following the manufacturer's instruction, the samples were observed under a microscope and imaged with a digital camera (Canon, EOS 350D, Tokyo, Japan).

Table 3 Grouping of osteogenic differentiation

Factor	Group			
	C1	C2	C3	C4
OIF	−	−	+	+
DCEF	−	+	−	+

Table 4 The primer sequences used for real-time PCR

Gene	Primer sequences
CXCR4	Forward: 5′-TGACGGACAAGTACAGGCTGC-3′ Reverse: 5′-CCAGAAGGGAAGCGTGATGA-3′
β-actin	Forward: 5′-ATATCGCTGCGCTCGTCGTC-3′ Reverse: 5′-CCTTGGGTCAGGTTTAGAG-3′
RUNX2	Forward: 5′-CCCGTGGCCTTCAAGGT-3′ Reverse: 5′-CGTTACCCGCCATGACAGTA-3′
ALP	Forward: 5′-CTGCCTACTTGTGTGGCGTGA-3′ Reverse: 5′-CCACCCATGATCACGTGCATA-3′

Quantitative real-time polymerase chain reaction

Following the exposure to DCEF and OIF, the expression of OPN and BSP in the cells were determined by rPCR. Primers were shown in Table 4. Briefly, rBMSCs at passage 3, which were divided into four groups described in Table 3, were harvested and isolated for RNA using the TRIzol Reagent (Invitrogen, USA). RNA was quantified by spectrophotometry. Approximately 1 μg of total RNA was reverse transcribed to cDNA using the Super Script First-Strand Synthesis Kit (Takara, Japan). Real-time polymerase chain reaction (PCR) reactions were performed using the SYBR Premix Dimer Eraser Kit (Takara, Japan) and the Applied Bio-Rad CFX96 Real-Time PCR Detection System (Bio-Rad, USA). Three independent experiments were conducted, and each reaction was run in triplicate.

Protein isolation and western blot analysis

As described above, the expression for osteogenesis-related proteins was determined by western blot analysis. To study protein regulation by exposure to DCEF and OIF, the third generation of BMSCs was divided into four groups in Table 3. Cells used in the experiment were collected at the same time and under the same conditions but from multiple batches in 24-well plates, and then the total cells were washed with ice-cold PBS and scraped in RIPA lysis buffer (Beyotime, China) including protease inhibitors. Equal amounts per sample of cell lysates (40–50 μg) were subjected to 10% SDS-PAGE and then transferred to a polyvinylidene fluoride (PVDF) membrane (Millipore, USA). The membranes were blocked with 5% bovine serum albumin (BSA) for 1 h at room temperature. Primary antibodies were incubated with tris-buffered saline and Tween 20 (TBST) containing 5% nonfat milk overnight at 4 °C, which included primary polyclonal antibodies against anti-rabbit ALP (1:1000; Abcam, USA), anti-rabbit RUNX2 (1:2000; Abcam, USA), and anti-rabbit CXCR4 (1:800; Abcam, USA), and anti-rabbit β-actin (1:1000; Sigma, USA). Monoclonal primary antibodies against β-actin was purchased from Abcam, USA. After washing with TBST, the immune complexes on the membranes were incubated with HRP-conjugated anti-rabbit IgG&H secondary antibodies (ab6734, Abcam, USA). Immunodetection was conducted using the Chemi-Doc™ MP System (1708280, Bio-Rad, USA). The relative intensity of immunoreactive bands was analyzed using Image J software.

Statistical analysis

SPSS for Windows (version 16.0) was used for statistical analysis. Data were expressed as mean ± standard deviation. Student's t test and one-way ANOVA were adopted for all statistical data. $P < 0.05$ was considered statistically significant.

Results

Culture, differentiation, and characterization of rBMSCs

The rBMSCs were healthy and displayed a uniform spindle shape (Fig. 2A). The results showed that the rBMSCs can

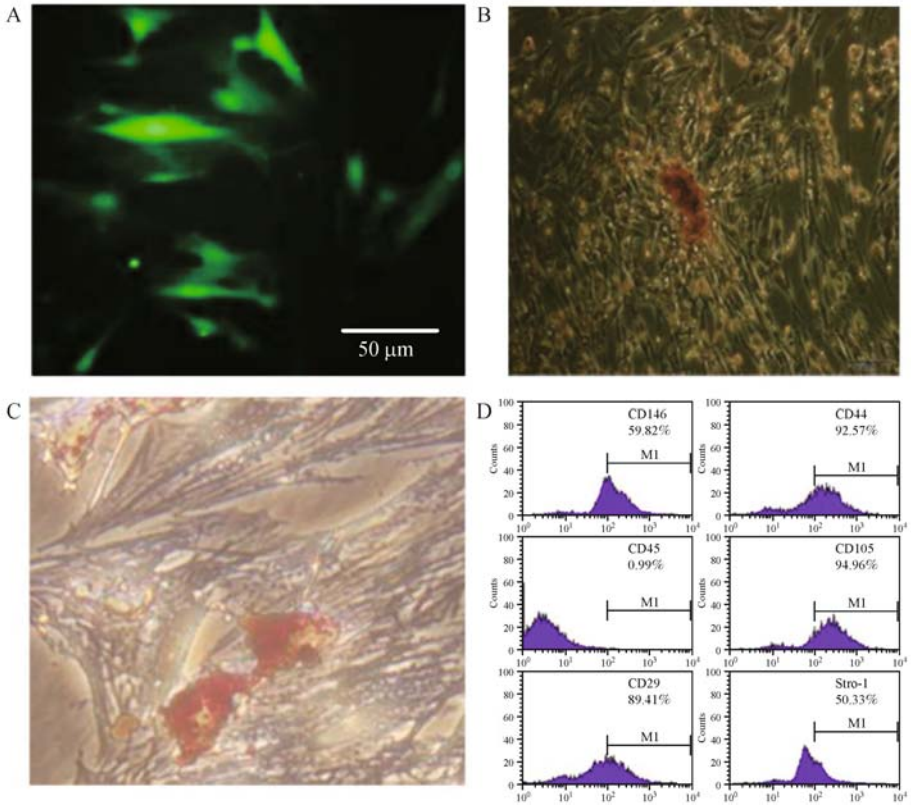

Fig. 2 rBMSCs culture, differentiation, and characterization. (A) The third generation of rBMSCs displayed in spindle shape (100 ×). (B and C) The third generation of rBMSCs differentiated into osteogenic and adipogenic lineages by oil red O staining and Alizarin Red S. (D) Flow cytometric analysis showed that rBMCSs were positive for CD44, CD105, CD29, CD146, and Stro-1 but negative for CD45.

differentiate into osteogenic and adipogenic cells (Fig. 2B and 2C). The phenotypic characterization conducted using flow cytometric analysis (Fig. 2D) showed that rBMSCs were positive for mesenchymal stem cell markers CD29, CD105, CD44, CD146, and Stro-1 but negative for markers CD45, which is consistent with previous reports [16].

Effects of DCEF on the direction of rBMSCs migration

The third-generation rBMSCs were divided into three experimental groups (Table 1). The number of cells migrating to the lower chamber in group A2 (with positive electrode at the top and negative electrode at the bottom) was lower compared with group A1 (without DCEF) (27.67 ± 3.79 vs. 17.00 ± 2.65, $P < 0.05$). In group A3 (with negative electrode at the top and positive electrode at the bottom), the number of migrating cells had the highest migration response (42.33 ± 5.51 vs. 17.00 ± 2.65, $P < 0.05$). The results showed that DCEF influenced rBMSCs to migrate towards the positive electrode (Fig. 3A and 3B).

Migration of rBMSCs in response to DCEF of different intensities and durations

Without DCEF, the numbers of rBMSCs migrating to the lower chamber were 7.67 ± 0.58, 8.67 ± 1.16 and 9.00 ± 2.00 at 2, 4, and 6 h, respectively, and no significant differences between any of the groups were observed ($P > 0.05$). In the presence of DCEF at 100 mV/mm, the number of rBMSCs migrating to the lower chamber was time dependent. The number of migrating cells at 2 h was 8.67 ± 0.58, while the numbers of migrating cells at 4 h (8.67 ± 0.58 vs. 23.00 ± 1.00) and 6 h (28.33 ± 1.53 vs. 8.67 ± 0.58) were approximately three times higher than in the 2-h group, and these differences were statistically significant ($P < 0.05$). The number of migrating cells exposed to a DCEF of 200 mV/mm for 2 h was larger than those exposed to 100 mV/mm for 2 h (19.00 ± 2.00 vs. 8.67 ± 0.58, $P < 0.05$). The number of migrating cells exposed for 4 h to a DCEF of 200 mV/mm was similar to the group that was exposed to 200 mV/mm for 6 h (47.67 ± 8.51 vs. 48.00 ± 4.58, $P > 0.05$). The number of migrating cells exposed to a DCEF of 300 mV/mm for 2, 4, and 6 h was 21.33 ± 3.22, 48.33 ± 7.64, and 48.67 ± 5.51, respectively. The number of migrating cells exposed to a DCEF of 300 mV/mm for 4 h was larger than those exposed to 300 mV/mm for 2 h (48.33 ± 7.64 vs. 21.33 ± 3.22, $P < 0.05$) (Fig. 3C and 3D). Statistical analysis showed that there was no significant difference between the 200 mV/mm for 4 h, 200 mV/mm for 6 h, 300 mV/mm for 4 h, and 300 mV/mm for 6 h groups ($P > 0.05$).

DCEF increased the proliferation rate of rBMSCs

Despite the cells being exposed to DCEF, rBMSCs underwent logarithmic growth for 3 of the 5 days on the platform. DCEF of 200 mV/mm for 4 h led to an increase in rBMSCs proliferation ability beyond the logarithmic growth period compared with the rBMSCs that were not exposed to DCEF (3 days, 0.821 ± 0.089 vs. 0.684 ± 0.037; 4 days, 0.900 ± 0.043 vs. 0.753 ± 0.090; 5 days, 1.080 ± 0.025 vs. 0.942 ± 0.009; 6 days, 1.119 ± 0.020 vs. 0.990 ± 0.031; 7 days, 1.111 ± 0.024 vs. 1.010 ± 0.011) (Fig. 3E).

Cells in the presence of the PI fluorescence were detected using Beckman counter flow cytometer, and the percentage of positive cells was recorded. In the experiment, 85.48% of the cells in the control group were in G_1 phase, and 79.23% of the cells in DCEF were in G_1 phase. This result suggested that both cell groups had good proliferation and differentiation potentials. In addition, the percentage of cells in G_2 and S phases were higher in the DCEF group than that in the control group (18.3% vs. 7.8% and 3.72% vs. 1.97%), which suggested that DCEF promote the proliferation rate of rBMSCs effectively (Fig. 3F and 3G).

Effects of DCEF on osteogenic ability of rBMSCs

The results of ALP staining experiment showed that group C4 (under DCEF and with OIF) had the largest volume of osteogenesis nodules, followed by C3 (with OIF), C2 (under DCEF), and C1 (with neither DCEF nor OIF) groups, respectively. These results showed that DCEF was effective in accelerating the osteogenic differentiation, but had less effect than OIF (Fig. 4C and 4D).The protein and gene expressions were congruent with ALP staining. The result also showed that DCEF can promote osteogenetic gene expression, including BSP and OCN (Fig. 4E). The protein expressions of ALP and RUNX2 were upregulated as well (Fig. 4A and 4B).

Influence of SDF-1/CXCR4 on migration of rBMSCs treated with DCEF

The rBMSCs in group B5 (with SDF-1 and under DCEF) had the highest number of migrating cells, which was significantly higher than group B2 (with SDF-1 but without DCEF) (99.33 ± 8.26 vs. 69.00 ± 8.72, $P < 0.01$). To further confirm whether DCEF strengthens rBMSCs mobilization via upregulation of SDF-1/CXCR4, rBMSCs were pretreated with SDF-1/CXCR4 cascade antagonist AMD3100 to block SDF-1 binding to CXCR4. As expected, in group B3 (with SDF-1, DCEF, and AMD3100), the number of migrating cells was significantly less than in group B5 (47.00 ± 4.00 vs.

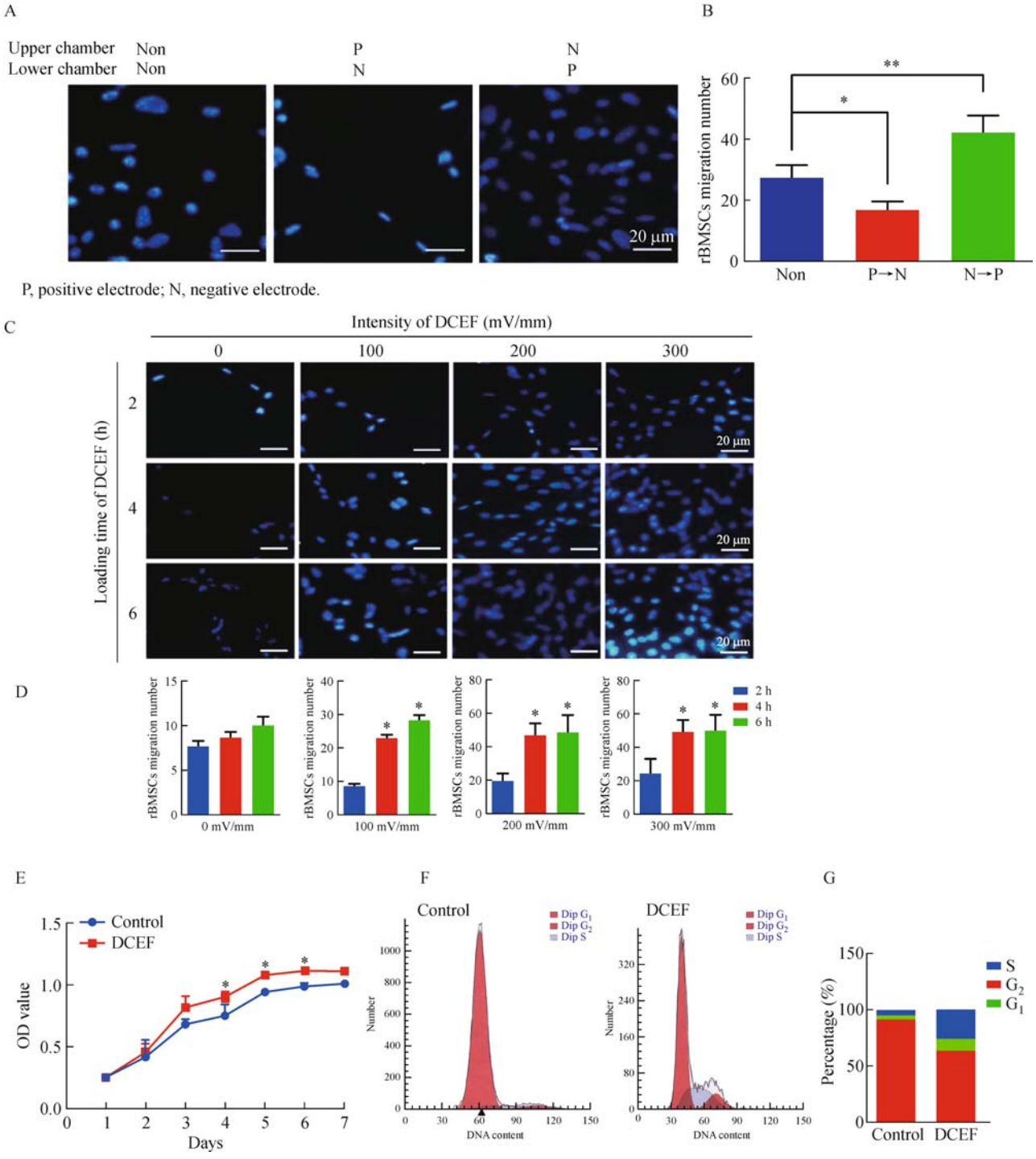

Fig. 3 Direct current electric field stimulation. (A) Effects of DCEF on rBMSCs migration direction. The amounts of rBMSCs migrating to the lower chamber in DCEFs of different polar patterns. (B) Results of intensity and loading time screening. Data was the number of experimental migrated cells relative to the control group. (C) Migration of rBMSCs in response to DCEF of different intensities and loading durations. The range of loaded time is from 0 to 6 h, and the range of intensity is from 0 to 300 mV/mm. The nonmigrating rBMSCs were removed, and the migrated cells were stained with DAPI followed by observation under a fluorescence microscope. Transwell chamber assay showed that DCEF promoted rBMSCs migration (20 ×). (D) Relative percentage of experimental migrated cells in the experimental as compared with the normal group. (E) Growth curve showed the effect of the DCEF on the proliferation of rBMSCs. (F) rBMSCs were exposed in DCEF after which cell cycle analysis was performed with flow cytometer. The control group: the result of cell cycle and proliferation index without the DCEF. G_1, 91.97%; G_2, 3.04%; S, 4.98%. The DCEF group: the result of cell cycle and proliferation index with the DCEF. G_1, 63.91%; G_2, 10.37%; S, 25.72%. (G) Percentage of cell cycle analysis by flow cytometry. $^*P < 0.05$ vs. non-group, $^{**}P < 0.01$ vs. non-group, Student's *t* test.

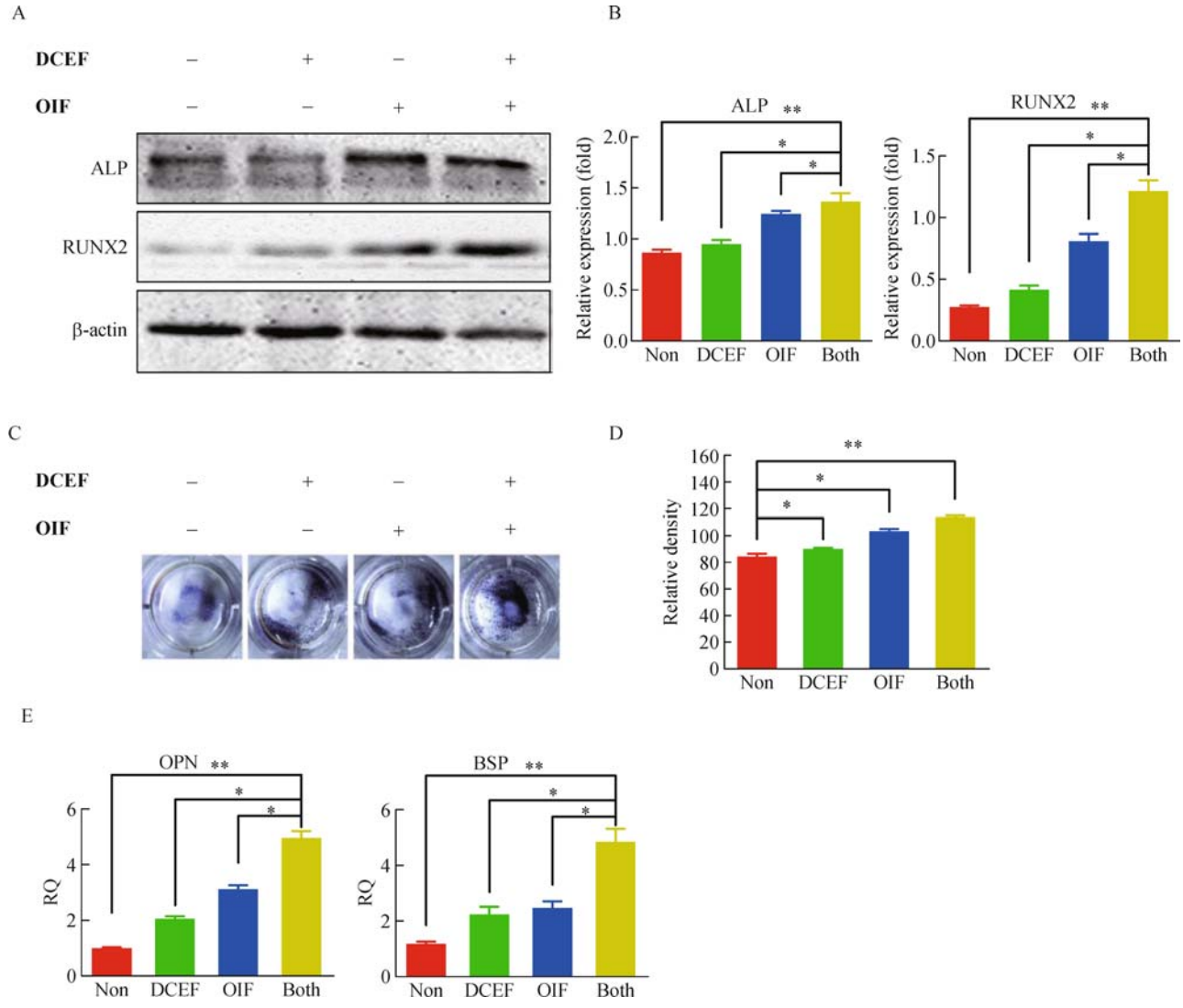

Fig. 4 Protein expression and gene expression in rBMSCs under DCEF. (A) Two kinds of influential factors were added to the culture of rBMSCs. Western blot analysis and scanning densitometer of ALP and RUNX2 expression in rBMSCs under DCEF. (B) Relative expression change of ALP and RUNX2. (C) ALP activation indicated differences in osteogenesis. (D) Relative density change of osteogenesis. (E) Real-time PCR analysis of OCN and BSP expression in rBMSCs under DCEF. *$P < 0.05$ vs. control group, **$P < 0.01$ vs. control group, Student's t test. +, this variable was applied; –, this variable was not applied.

99.33 ± 8.26, $P < 0.01$), while it was slightly increased in group B6 (with SDF-1 and AMD3100) (47.00 ± 4.00 vs. 31.33 ± 4.16, $P < 0.05$) (Fig. 5A and 5B). Additionally, the protein expression of CXCR4 had significantly increased under DCEF (Fig. 5C and 5D).

Discussion

BMSC migration into the wound is an essential part of bone healing in mammals. Endogenic DCEF is a powerful directional cue that directs various types of cells, including keratinocytes, epithelial cells, fibroblasts, vascular endothelial cells, osteoblasts, neural stem cells, and MSCs, to migrate toward a wound area [17–20]. Exogenous DCEF, which is more stable and modifiable, constitutes a novel tool to force polarization and migration of BMSCs in bone tissue engineering and healing.

When treated with DCEF, the cells' migration, whether toward the cathode or toward the anode, is highly dependent on the specific cell type. As to the electrotaxis of the MSCs and the osteoblasts, conflicting results are found in previous published articles. Zhao *et al.* showed that mouse ASCs and rat MSCs migrated toward the cathode, whereas human MSCs, human iPS, and human osteoblasts migrated toward the anode. Other studies

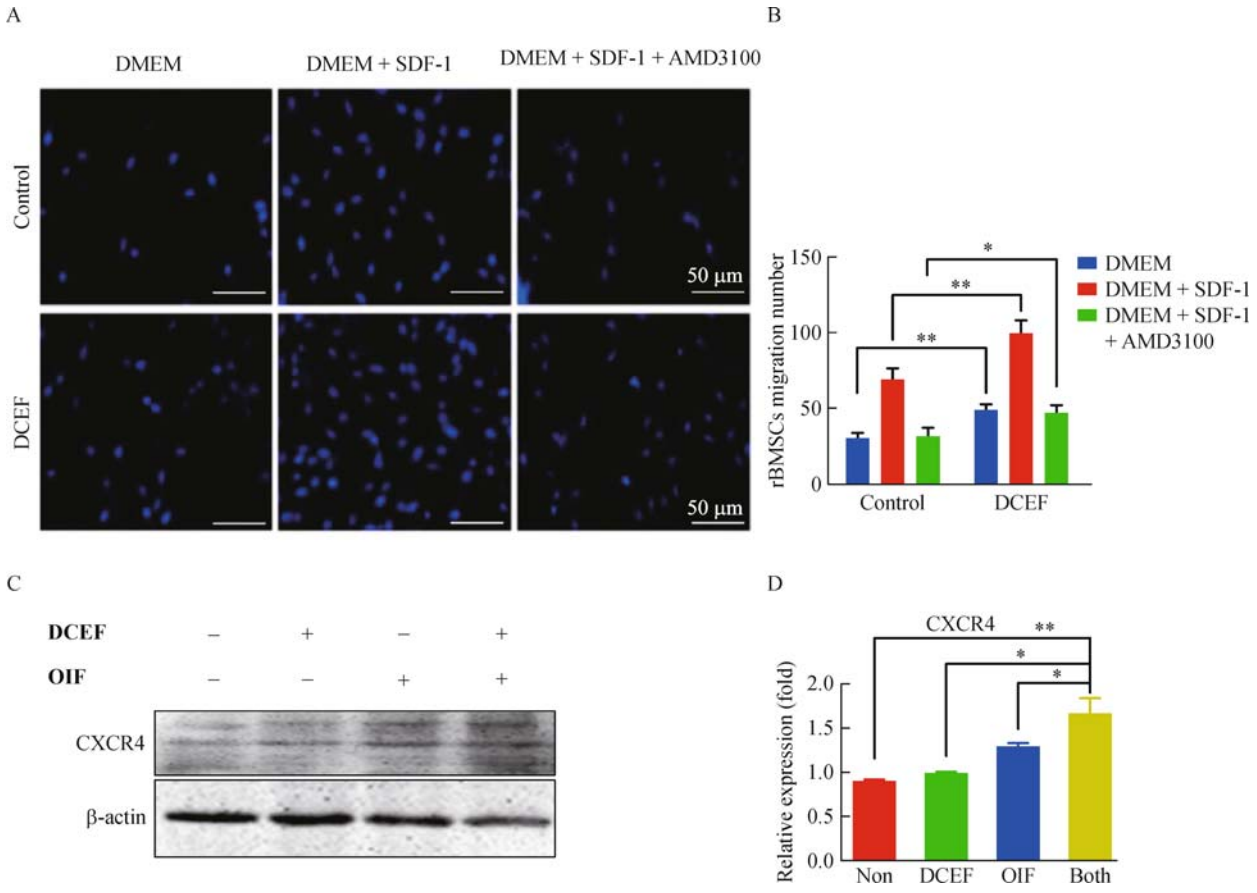

Fig. 5 SDF-1/CXCR4 axis influences rBMSCs migration. The nonmigrating rBMSCs were removed and the migrated cells were stained with DAPI followed by observation under a fluorescence microscope. (A) Transwell chamber assay showed that SDF-1 promoted rBMSCs migration, which could be inhibited by AMD3100 in DCEF (100 ×). (B) Relative percentage of experimental migrated cells in experimental as compared with control group. Result is the summary of the six separate experiments. (C) Western blot analysis and scanning densitometer of CXCR4 expression in rBMSCs. (D) Relative expression of CXCR4. *$P < 0.05$ vs. non-group, **$P < 0.01$ vs. non-group, Student's t test. +, this variable was applied; −, this variable was not applied.

showed that rat osteoblasts migrated toward the cathode [21,22]. These findings indicated that rBMSCs showed significant anode-directed migration at a very commonly used DCEF strength at 200 mV/mm, a widely used DCEF strength globally. The differences in cell types, tissue sources, and DCEF equipment may contribute to these differences in electrotaxis of similar cells.

In this study, a comparison of the intensity and loading duration of DCEF was conducted *in vitro* using the Transwell migration assay, which was commonly used to study the migratory response of a variety of cell types to inducing or inhibitory agents. The rBMSCs were cultured in the upper chamber on a layer of Matrigel fibronectin that was coated on the microporous membrane between the upper and lower chambers. The rBMSCs in the upper chamber migrated into the lower chamber due to the electrotaxis effect of the DCEF. The present study revealed that when a DCEF of 200 mV/mm was applied for 4 h, 60% of rBMSCs moved to the lower chamber. Additional experiments were performed to study the influence of the DCEF on the osteogenic differentiation and proliferation of the rBMSCs. The results showed that a DCEF of 200 mV/mm for 4 h was optimal in strength and duration for facilitating migration, proliferation, and osteogenic differentiation of rBMSCs. The optimal DCEF strength determined by experiments done in the present paper was similar to those of Zhao and Luo [23], as well as the strength used in some *in vitro* studies [24]. The results of the present paper showed that the optimal DCEF duration was 4 h, while varying results ranging from 2 to 6 h were found in previous studies. In the present study, although the rBMSCs, exposed to a DCEF of 300 mV/mm for 4 h, 200 mV/mm for 6 h, or 300 mV/mm for 6 h, had similar migratory rates as rBMSCs exposed to a DCEF of 200 mV/mm for 4 h, the present paper recommend the DCEF of 200 mV/mm because it is closer to the strength of endogenous EF.

Reports have pointed out that some cells, such as neural

precursor cells and bone marrow mesenchymal stem cells, under the action of electric field can be activated following injury, resulting in their proliferation and migration toward injury sites where they differentiate into mature cells [25]. The surrounding tissue only is usually impacted, but not the whole body. The present study suggested the intensity of the electric field to be ideal options as it promoted cell migration effectively. Thus, external application of DCEF may act as a cue to direct migration of rBMSCs in bone regeneration and repair. The present study also examined the expression of some key molecules related to osteogenic capability, such as ALP, RUNX2, OPN, and BSP. ALP is an early marker of osteogenic differentiation which can be hydrolyzed to release inorganic phosphate. The expression level of ALP increased to a certain extent, reflecting the ability of the cells to enhance osteogenesis [26]. RUNX2 is essential for osteoblastic differentiation and the bone formation and maintenance [27]. It plays an important role in terminal differentiation. In addition, osteogenic genes, including OPN and BSP, are the abundant noncollagenous proteins in the extracellular matrix of the bone tissue [28]. These two genes have been shown to be crucial to the formation of bone, regulating both bone cell mineralization and attachment [29]. Through this study, it was implicated that DCEF indeed increased in both gene and protein expressions. Further study is required to elucidate the mechanisms why osteogenesis which was induced by rBMSCs occurred in the presence of the electric field.

The SDF-1/CXCR4 axis has been shown to play important roles in migration, proliferation, differentiation, and bone development [30]. Using mouse segmental bone graft models, Luan *et al.* [31] demonstrated that the SDF-1/CXCR4 axis plays a critical role in the recruitment of MSCs on the site of bone healing which contributes to endochondral bone repair. Previous studies have shown that early deletion of the CXCR4 gene in osteoblastogenesis disrupts osteoblast formation and bone development [32]. It has been reported that SDF-1/CXCR4 signaling in the mature osteoblast can feedback to regulate the osteoclast precursor pool size and play a multifunctional role in regulating bone formation and resorption [33]. SDF-1 might induce cell migration to the injury area, which is consistent with the results of the present study. This selective homing indicated that DCEF could recruit rBMSCs to the bone injury to participate in osteogenesis, which suggests that a similar effect occur with endogenous stem cells.

Though it is not clear that the DCEF-dependent mechanism promotes osseointegration and bone remodeling, the cellular recruitment noted in the present study may be a consequence of elevated expression of various growth factors and cytokines induced by DCEF. From Fig. 5, it is clear that SDF-1/CXCR4 is involved in the rBMSC migration induced by DCEF, but targeting the CXCR4/SDF-1 axis alone is insufficient to inhibit DCEF-mediated migration. Other molecules, such as PI3 kinase, PTEN, EGFR, ERK1/2, cAMP, and Rho small GTPases may also mediate the electrotactic response of rBMSCs [34]. The present paper hypothesize that the influence of DCEF on osseointegration is possible through changes in the phosphoinositide signaling pathway, among other factors. Moreover, the CXCR7/SDF-1/ITAC axis, which includes the SDF-1 receptor CXCR7, may also be involved in rBMSC migration [35].

Conclusions

The present study provided evidence about the role of DCEF in the directional migration of rBMSCs. A DCEF of 200 mV/mm for 4 h can enhance the migration, proliferation, and osteogenic differentiation of rBMSCs. The SDF-1/CXCR4 signaling axis is involved in the rBMSC migration mediated by DCEF.

Acknowledgements

This study was supported by the Chinese Army Five-Year Project Funding (CWS12J134) and the National Natural Science Foundation of China (No. 51473175). We appreciate the Chinese Academy of Agricultural Sciences and the Institute of Orthopedics for their assistance for our experiments.

Compliance with ethics guidelines

Xiaoyu Wang, Yuxuan Gao, Haigang Shi, Na Liu, Wei Zhang, and Hongbo Li declare that they have no conflict of interest. All institutional and national guidelines for the care and use of laboratory animals were followed.

References

1. Derubeis AR, Cancedda R. Bone marrow stromal cells (BMSCs) in bone engineering: limitations and recent advances. Ann Biomed Eng 2004; 32(1): 160–165
2. Kumar A, Nune KC, Misra RD. Electric field-mediated growth of osteoblasts — the significant impact of dynamic flow of medium. Biomater Sci 2016; 4(1): 136–144
3. De Bari C, Dell'Accio F, Vandenabeele F, Vermeesch JR, Raymackers JM, Luyten FP. Skeletal muscle repair by adult human mesenchymal stem cells from synovial membrane. J Cell Biol 2003; 160(6): 909–918
4. Fong EL, Chan CK, Goodman SB. Stem cell homing in musculoskeletal injury. Biomaterials 2011; 32(2): 395–409
5. Korohoda W, Grys M, Madeja Z. Reversible and irreversible electroporation of cell suspensions flowing through a localized DC electric field. Cell Mol Biol Lett 2013; 18(1): 102–119
6. Vanegas-Acosta JC, Garzón-Alvarado DA, Lancellotti V. Numerical simulation of electrically stimulated osteogenesis in dental implants. Bioelectrochemistry 2014; 96: 21–36

7. Funk RH, Monsees T, Ozkucur N. Electromagnetic effects: from cell biology to medicine. Prog Histochem Cytochem 2009; 43 (4):177–264
8. Zhao M. Electrical fields in wound healing—an overriding signal that directs cell migration. Semin Cell Dev Biol 2009; 20(6): 674–682
9. Chiang M, Robinson KR, Vanable JW Jr. Electrical fields in the vicinity of epithelial wounds in the isolated bovine eye. Exp Eye Res 1992; 54(6): 999–1003
10. Zhao Z, Watt C, Karystinou A, Roelofs AJ, McCaig CD, Gibson IR, De Bari C. Directed migration of human bone marrow mesenchymal stem cells in a physiological direct current electric field. Eur Cell Mater 2011; 22: 344–358
11. Lee JW, Lee J, Moon EY. HeLa human cervical cancer cell migration is inhibited by treatment with dibutyryl-cAMP. Anticancer Res 2014; 34(7): 3447–3455
12. Pullar CE, Isseroff RR. Cyclic AMP mediates keratinocyte directional migration in an electric field. J Cell Sci 2005; 118(Pt 9): 2023–2034
13. Finkelstein E, Chang W, Chao PH, Gruber D, Minden A, Hung CT, Bulinski JC. Roles of microtubules, cell polarity and adhesion in electric-field-mediated motility of 3T3 fibroblasts. J Cell Sci 2004; 117(Pt 8): 1533–1545
14. Pullar CE, Isseroff RR, Nuccitelli R. Cyclic AMP-dependent protein kinase A plays a role in the directed migration of human keratinocytes in a DC electric field. Cell Motil Cytoskeleton 2001; 50(4): 207–217
15. Shichinohe H, Kuroda S, Yano S, Hida K, Iwasaki Y. Role of SDF-1/CXCR4 system in survival and migration of bone marrow stromal cells after transplantation into mice cerebral infarct. Brain Res 2007; 1183: 138–147
16. Pittenger MF, Mackay AM, Beck SC, Jaiswal RK, Douglas R, Mosca JD, Moorman MA, Simonetti DW, Craig S, Marshak DR. Multilineage potential of adult human mesenchymal stem cells. Science 1999; 284(5411): 143–147
17. McCaig CD, Song B, Rajnicek AM. Electrical dimensions in cell science. J Cell Sci 2009; 122(Pt 23): 4267–4276
18. Yao L, McCaig CD, Zhao M. Electrical signals polarize neuronal organelles, direct neuron migration, and orient cell division. Hippocampus 2009; 19(9): 855–868
19. Zhao Z, Qin L, Reid B, Pu J, Hara T, Zhao M. Directing migration of endothelial progenitor cells with applied DC electric fields. Stem Cell Res (Amst) 2012; 8(1): 38–48
20. Hammerick KE, Longaker MT, Prinz FB. *In vitro* effects of direct current electric fields on adipose-derived stromal cells. Biochem Biophys Res Commun 2010; 397(1): 12–17
21. Ferrier J, Ross SM, Kanehisa J, Aubin JE. Osteoclasts and osteoblasts migrate in opposite directions in response to a constant electrical field. J Cell Physiol 1986; 129(3): 283–288
22. Özkucur N, Monsees TK, Perike S, Do HQ, Funk RH. Local calcium elevation and cell elongation initiate guided motility in electrically stimulated osteoblast-like cells. PLoS ONE 2009; 4(7): e6131
23. Luo XF, Huang Y, Fan P, Peng B, Liu R, Bai H. Directed migration and morphological changes of cultured trophoblast cells in small electric fields. J Sichuan Univ (MedSci Edition) (Sichuan Da Xue Xue Bao Yi Xue Ban) 2010; 41(5): 771–774, 802 (in Chinese)
24. Zhang J, Neoh KG, Hu X, Kang ET, Wang W. Combined effects of direct current stimulation and immobilized BMP-2 for enhancement of osteogenesis. Biotechnol Bioeng 2013; 110(5):1466–1475
25. Gamboa OL, Pu J, Townend J, Forrester JV, Zhao M, McCaig C, Lois N. Electrical estimulation of retinal pigment epithelial cells. Exp Eye Res 2010; 91(2): 195–204
26. de Oliveira GL, de Lima KW, Colombini AM, Pinheiro DG, Panepucci RA, Palma PV, Brum DG, Covas DT, Simões BP, de Oliveira MC, Donadi EA, Malmegrim KC. Bone marrow mesenchymal stromal cells isolated from multiple sclerosis patients have distinct gene expression profile and decreased suppressive function compared with healthy counterparts. Cell Transplant 2015; 24(2): 151–165
27. Siddiqui S, Arshad M. Osteogenic potential of punica granatum through matrix mineralization, cell cycle progression and runx2 gene expression in primary rat osteoblasts. Daru 2014; 22(1): 72
28. Fernández I, Tiago DM, Laizé V, Leonor Cancela M, Gisbert E. Retinoic acid differentially affects *in vitro* proliferation, differentiation and mineralization of two fish bone-derived cell lines: different gene expression of nuclear receptors and ECM proteins. J Steroid Biochem Mol Biol 2014; 140: 34–43
29. Gordon JA, Tye CE, Sampaio AV, Underhill TM, Hunter GK, Goldberg HA. Bone sialoprotein expression enhances osteoblast differentiation and matrix mineralization *in vitro*. Bone 2007; 41(3): 462–473
30. Yilmaz G, Hwang S, Oto M, Kruse R, Rogers KJ, Bober MB, Cahill PJ, Shah SA. Surgical treatment of scoliosis in osteogenesis imperfecta with cement-augmented pedicle screw instrumentation. J Spinal Disord Tech 2014; 27(3): 174–180
31. Luan J, Cui Y, Zhang Y, Zhou X, Zhang G, Han J. Effect of CXCR4 inhibitor AMD3100 on alkaline phosphatase activity and mineralization in osteoblastic MC3T3-E1 cells. Biosci Trends 2012; 6(2): 63–69
32. Hronik-Tupaj M, Rice WL, Cronin-Golomb M, Kaplan DL, Georgakoudi I. Osteoblastic differentiation and stress response of human mesenchymal stem cells exposed to alternating current electric fields. Biomed Eng Online 2011; 10(1): 9
33. Kawakami Y, Ii M, Matsumoto T, Kuroda R, Kuroda T, Kwon SM, Kawamoto A, Akimaru H, Mifune Y, Shoji T, Fukui T, Kurosaka M, Asahara T. SDF-1/CXCR4 axis in Tie2-lineage cells including endothelial progenitor cells contributes to bone fracture healing. J Bone Miner Res 2015; 30(1): 95–105
34. Leppik LP, Froemel D, Slavici A, Ovadia ZN, Hudak L, Henrich D, Marzi I, Barker JH. Effects of electrical stimulation on rat limb regeneration, a new look at an old model. Sci Rep 2015; 5: 18353
35. Grymula K, Tarnowski M, Wysoczynski M, Drukala J, Barr FG, Ratajczak J, Kucia M, Ratajczak MZ. Overlapping and distinct role of CXCR7-SDF-1/ITAC and CXCR4-SDF-1 axes in regulating metastatic behavior of human rhabdomyosarcomas. Int J Cancer 2010; 127(11): 2554–2568